Contents lists available at SciVerse ScienceDirect

Chemical Engineering Journal

journal homepage: www.elsevier.com/locate/cej

Aerosol processing of low-cost mesoporous silica spherical particles from photonic industrial waste powder for CO_2 capture

Liang-Yi Lin, Hsunling Bai *

Institute of Environmental Engineering, National Chiao Tung University, Hsinchu 300, Taiwan

HIGHLIGHTS

▶ Mesoporous silica particle, MSP (AS) was synthesized via aerosol spray method.
▶ Using photonic waste and inorganic salt as precursors reduces the chemical costs.
▶ MSP (AS) made from photonic waste can be a potential adsorbent for CO_2 capture.

ARTICLE INFO

ABSTRACT

A novel mesoporous silica spherical particle, MSP (AS) was facilely prepared using photonic industrial waste powder as the silica source via salt-templated aerosol spray approach. As an alternative to expensive mesoporous silica materials in prior works, the obtained MSP (AS) possesses advantages of simple and rapid synthesis with low manufacturing costs. The characteristics of the MSP (AS) material were investigated by the XRD, N_2 adsorption–desorption measurement, SEM, TEM and TG/DTG analyses. The results clearly demonstrated the presence of mesoporous siliceous material with high specific surface area (585 m^2/g), mesopore size (9.1 nm) as well as large pore volume (1.24 cm^3/g). Furthermore, the MSP (AS) is evaluated as the support of adsorbent in terms of CO_2 adsorption. It is observed that the amine-functionalized MSP (AS) adsorbent (TEPA-MSP (AS)) which possessed larger pore diameter and pore volume tends to have a higher adsorption capacity of 127 mg CO_2/g adsorbent. This is superior to those of TEPA-SBA-15 (117 mg CO_2/g adsorbent), TEPA-MCM-41 (112 mg CO_2/g adsorbent) and TEPA-NaY (96 mg CO_2/g adsorbent) under the same test condition. The results clearly suggest that the MSP (AS) synthesized using photonic industrial solid wastes via salt-templated aerosol route can be a potential and cost-effective adsorbent for CO_2 capture.

© 2012 Elsevier B.V. All rights reserved.

1. Introduction

Over the last years, the carbon dioxide capture and storage (CCS) is considered to be feasible approach which can effectively limit the CO_2 emissions from power plants and industrial processes [1]. Among various processes, amine-functionalized solid adsorbent for CO_2 adsorption is getting great attention because of its high performance and simplicity of regeneration [2]. To this end, possible dry adsorbents including silica-gel [3], activated carbons [4], carbon nanotubes [5], metal oxides [6] and zeolite materials [7] have been widely investigated on CO_2 adsorption in terms of adsorption capacity, regeneration ability and tolerance under water-existing environment.

Recent advances in the development of efficient amine-functionalized adsorbents revealed that amine molecules can be introduced and stabilized insides the pore channels of the mesoporous silica materials leading to high adsorption performance [8]. Owning to their characteristic of high surface area, tunable pore sizes, well-defined pore structure and unique surface chemistry via functionalization, these mesoporous silica materials are considered as ideal adsorbents and supports. Son et al. [9] employed a series of amine-impregnated mesoporous silica materials, including MCM-41, MCM-48, SBA-15, SBA-16 and KIT-6 for CO_2 adsorption. The results clearly demonstrated that these amine-impregnated mesoporous silica materials are potential CO_2 adsorbents due to their high adsorption capacity, fast mass transfer kinetics and ease of regeneration.

Numerous reports have demonstrated the preparation of mesoporous silica by a variety of silica sources including silicon alkoxides and fumed silica, along with organic surfactants like $C_{16}H_{33}(CH_3)_3$ NBr (CTAB) as the structure-directing template [10,11]. However,

* Corresponding author. Address: Institute of Environmental Engineering, National Chiao Tung University, 1001 University Rd., Hsinchu 300, Taiwan. Tel.: +886 3 5731868; fax: +886 3 5725958.
E-mail address: hlbai@mail.nctu.edu.tw (H. Bai).

the high manufacturing costs due to the preferred silica sources and organic surfactants might prevent cost-effective and large-scale production of the mesoporous materials to replace industrially manufactured zeolite materials. The use of cheaper starting precursors in the manufacturing process would be a great contribution to industrial applications, especially for the capture of abundant CO_2 greenhouse gas where massive quantities of adsorbents are required.

One of the promising approaches to prepare low-cost mesoporous adsorbents is the replacement of commercial chemicals with waste products as the starting precursor. Recent years, the reutilization of silicon-containing waste products such as coal fly ash [12], rice husk ash [13–15] and blast-furnace slag [16] for the fabrication of microporous and/or mesoporous materials have been successfully conducted. This would be expected to be economically beneficial in industrial manufacture of huge amount of adsorbents. Our prior study investigated the feasibility of extracting silicate supernatant from the photonic industrial waste powder, which is one of the major by-products in semiconductor and photonic industries [17]. It was demonstrated that the photonic waste powder could be an alternative resource for producing silica-based materials.

Up to date, most researches on the synthesis of mesoporous silica materials from siliceous wastes has been processed through solution precipitation methods using batch reactors, which require complex preparation steps and long contact times. To overcome the disadvantages of traditional batch processes, vapor-phase synthesis of the mesoporous silica materials has been recently developed and become one of the facile processes for particles engineering purposes due to its rapid and continuous synthesis as well as simplicity of scaling up [18–24]. However, to the authors' knowledge, there is no report yet concerning the synthesis of mesoporous silica materials via aerosol approach using industrial solid wastes as the starting material.

In the present study, attempts have been made to utilize photonic industrial waste powder as the silicon source to synthesize mesoporous silica particles (MSPs) by aerosol spray approach for the first time. The inorganic salt of $(NH_4)_2SO_4$ is driven to replace the traditional organic surfactants as a template to support the formation of the mesoporous network. The crystalline composition, pore structure, morphology and thermal stability of the obtained MSPs are presented. Moreover, the CO_2 adsorption performance of obtained MSPs is also evaluated and compared to that of the typical microporous and mesoporous silica materials including MCM-41, SBA-15 and commercial zeolite NaY adsorbent.

2. Experimental section

2.1. Synthesis of MSP (AS)

Fig. 1 depicts the experimental setup of the reactor for continuously synthesizing MSP materials via aerosol spray method using waste-derived silicate supernatant as the silica precursor and $(NH_4)_2SO_4$ was employed as the templating medium. The sodium silicate solution was prepared by mixing photonic waste powder with 6 M NaOH solution at room temperature for 12 h. Table 1 shows the elemental analysis of the raw waste powder and the silicate supernatant after extraction with NaOH solution. The molar composition of the precursor mixture was 1 SiO_2:3 $(NH_4)_2SO_4$:359 H_2O:7.32 HCl. The precursor mixture was mixed and nebulized by an ultrasonic atomizer and carried by a high pressure, clean and dry air flow. The reagent flow was then passed through a high-temperature tubular reactor with the temperature of 400 °C. The total flow rate in this study was fixed at 2000 cm^3/min (25 °C, 1 atm), which corresponded to a residence time of 4 s. After the heating process, the as-synthesized MSP samples were collected downstream of the reactor by a high-efficiency filter. Finally, they were recovered by washing and filtration with DI water followed by drying in an oven at 110 °C. The aerosol processing of mesoporous silica sample from the waste powder in the presence of $(NH_4)_2SO_4$ template was denoted as MSP (AS), while the mesoporous silica sample from the waste powder in the absence of $(NH_4)_2SO_4$ template was named as MSP.

To investigate the effect of the support on the adsorption capacity of the adsorbent, mesoporous silica materials including MCM-41 and SBA-15 were synthesized as well. The synthesis of MCM-41 was performed using pure chemicals of sodium metasilicate nanohydrate ($Na_2SiO_3 \cdot 9H_2O$) and cetyltrimethylammonium bromide (CTAB) as the silica source and template, respectively. The molar composition of the gel mixture was 1 SiO_2:0.2 CTAB:120 H_2O:0.89 H_2SO_4. The resulting gel mixture was transferred into a Teflon coated autoclave and kept in an oven at 145 °C for 36 h. After cooling to room temperature, the resultant solid was recovered by filtration, washed with DI water and dried in an oven at 100 °C. Finally, the organic template was removed by using a muffle furnace in air at 550 °C for 6 h.

Mesoporous SBA-15 was synthesized using a tri-block copolymer, $EO_{20}–PO_{70}–EO_{20}$ (Pluronic P123, BASF) as the template and sodium silicate solution (~14% NaOH, ~27% SiO_2, Aldrich) as the silica source. The molar composition of the gel mixture was 1 SiO_2:0.01 P123:286 H_2O:0.7 H_2SO_4. For a typical synthesis, 2.01 g of P123 (dissolved in 20 g of DI water) was added to 100 g of 6 M H_2SO_4. After stirring for 1 h, 8 g of sodium silicate solution (dissolved in 50 g of DI water) was added to the above solution with continuous stirring for 15 min. The resultant mixture was aged at 100 °C for 24 h. The obtained solid product was filtered and washed with DI water, followed by drying in an oven at 60 °C. Finally, the complete removal of residual surfactants was carried out by using a muffle furnace at 500 °C in air for 6 h.

2.2. Characterization of MSP (AS)

The elemental analysis of the raw waste powder was determined by energy-dispersive X-ray spectroscopy in a scanning electron
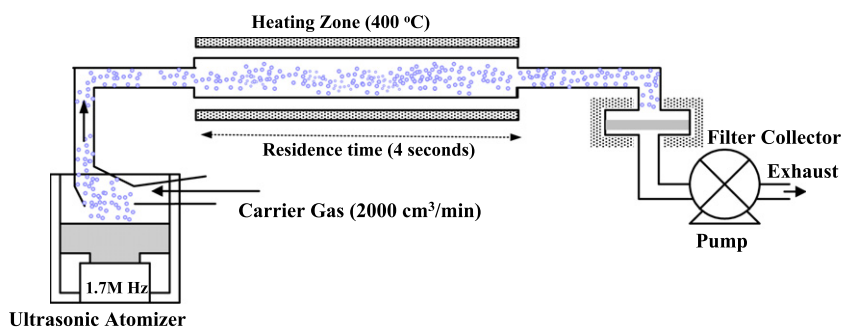

Fig. 1. Experimental setup for the generation of mesoporous silica spherical particles (MSPs) through aerosol spray process.

Table 1
Elemental analysis of photonic waste powder and silicate supernatant analyzed by the SEM-EDS and ICP-MS analysis.

Element	Si	F	O	N	Na
Photonic waste powder[a] (wt.%)	28.82	47.82	17.54	5.82	–
Supernatant[b] (ppm)	31,420	–	–[c]	–	69,670

[a] Sample analyzed by the SEM-EDS analysis.
[b] Sample analyzed by the ICP-MS analysis.
[c] Non-detected.

microscope (SEM-EDS, HITACHI-S4700). And the silicate supernatant was also analyzed by ICP-MS (SCIEX ELAN 5000 – Inductively Coupled Plasma-Mass Spectrometer). Powder angle X-ray diffraction patterns of mesoporous adsorbents were recorded by using Rigaku X-ray diffractometer equipped with nickel-filtered Cu Kα (λ = 1.5405 Å) radiation. The diffractograms of the mesoporous samples were recorded in the 2θ range 5–80° with a scanning speed of 4 degrees per minute. The specific surface area, pore volume and average pore diameter (BJH method) of the samples were measured by N_2 adsorption–desorption isotherms at −196 °C using a surface area analyzer (Micromeritics, ASAP 2000). The thermal behavior of the material was conducted in the temperature range of 25–900 °C by a thermo-gravimetric analyzer (TGA, Netzsch TG209 F1, Germany). The morphology of the material was observed via the SEM (HITACHI-S4700) images. TEM images of the samples were observed with a JEOL JEM 1210 TEM instrument operated at 120 keV and the samples (5–10 mg) were ultrasonicated in ethanol and dispersed on carbon film supported on copper grids (200 mesh).

### 2.3. CO₂ adsorption measurement

Amine-modified porous supports (MCM-41, SBA-15, MSP (AS) and NaY zeolite) were functionalized with tetraethylenepentamine (TEPA) at a weight ratio of 1:1 by the wet impregnation method reported by Lin and Bai [25]. The TEPA has been proved as an efficient reagent for the capture of CO_2. The CO_2 adsorption tests were conducted by a thermo-gravimetric analyzer (TGA, Netzsch TG209 F1, Germany). Typically, approximately 10 mg of adsorbents were loaded on the TGA sample holder and purged with nitrogen gas at the temperature of 110 °C with a flow rate of 120 cm³/min for 30 min until the weight is not changed, suggesting that the evaporation of water on the adsorbents was complete. The mass change of the adsorbents during CO_2 adsorption was then measured under isothermal condition of 60 °C. The inlet CO_2 concentration was 10% (v/v in N_2) which was obtained from a certified gas cylinder and introduced at a flow rate of 40 cm³/min (25 °C, 1 atm) for 60 min of adsorption time until the weight was not changed to ensure that the adsorbents were completely saturated. The moisture in the CO_2 gas cylinder was measured to be 5% relative humidity, which corresponded to an absolute moisture content of only 0.16% (v/v). This was much lower than the CO_2 concentration and thus the moisture impact on the CO_2 adsorption is negligible.

3. Results and discussion

3.1. Characterization of the MSP (AS)

Powder XRD patterns of the as-synthesized and washed MSP samples prepared using sodium silicate precursor from photonic waste powder through aerosol spray process are shown in Fig. 2. As can be seen from the results, the as-synthesized MSP sample prepared without $(NH_4)_2SO_4$ salt shows significant diffraction peaks at 2θ of 22°, 27°, 32°, 45°, 56°, 66° and 75°. The reflection peak centered at 22° can be assigned to the silica in amorphous phase and

the other peaks are indexed on the NaCl crystallite [26]. Since NaCl exhibits stronger crystallinity than that of amorphous silica, the NaCl crystallites are expected to show higher diffraction intensity as depicted in Fig. 2a. To elucidate the above findings, the general theory of silica polymerization must be addressed. In the preparation of silica precursors, two reactions took place simultaneously, i.e., condensation and sodium silicate acidification. The silica condensation process, which is the formation of a siloxane linkage between surface silanol groups, can be represented as [27]:

$$Si(OH)_4 + HO-Si(OH)_3 \rightarrow (OH)_3Si-O-Si(OH)_3 + H_2O \tag{1}$$
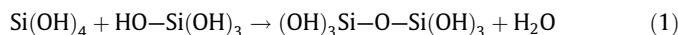
And the reaction of sodium silicate solution with hydrochloric acid during acidification process can be written as:

$$Na_2O \cdot xSiO_2 + 2HCl \rightarrow xSiO_2 \downarrow + 2NaCl + H_2O \tag{2}$$
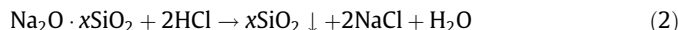
When the sodium silicate precursor is added to hydrochloric acid solution, fine crystallites of NaCl are formed and embedded in the silica particles during aerosol spray process. Consequently, the co-existence of amorphous silica and NaCl is observed in the as-synthesized MSP sample.

On the other hand, as the $(NH_4)_2SO_4$ salt is used in the starting precursors, the as-synthesized-MSP (AS) sample contains a large amount of crystalline $(NH_4)_2SO_4$ as the main component [28]. Meanwhile, the intensities of reflection peaks assigned to crystalline NaCl are decreased and become insignificant in the as-synthesized MSP (AS). This suggests that $(NH_4)_2SO_4$ is present with relatively higher loadings as compared to that of NaCl in the as-synthesized-MSP (AS) sample. After aqueous washing procedure, there is only one broad diffraction peak observed in the washed MSP (AS) material, which is indicative of amorphous silica [29]. This implies that pure siliceous material can be obtained after the removal of salt template by aqueous washing process.

To understand the thermal stability of the washed MSP (AS) material, the TGA and DTG analyses were carried out and shown in Fig. 3a and b, respectively. One can see from Fig. 3a that the washed MSP (AS) shows an initial weight loss at < 100 °C, which can be ascribed to the evaporation of the physically adsorbed water on the surface of the material. Besides, it is found from Fig. 3b that the DTG curve showed two weak peaks from 200 to 900 °C. The first step (200–600 °C) is due to the loss of chemically adsorbed water bonded to Si–OH through hydrogen bond. From 600 to 900 °C, the weight loss is expected to be associated with the further condensation of the Si–OH groups from the amorphous SiO_2 [30]. It is noticeable that there are no peaks assigned to the
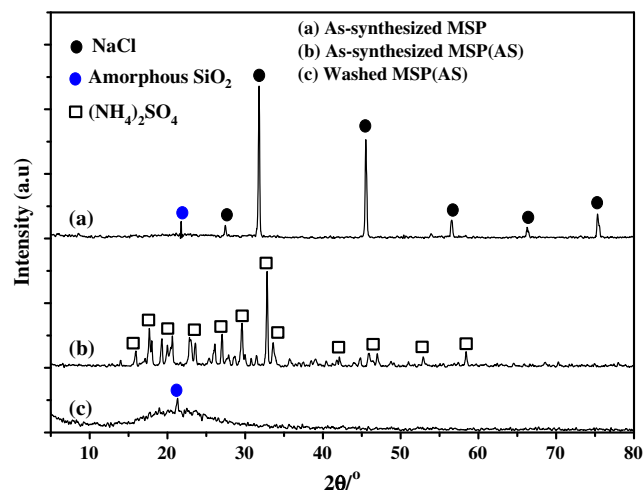

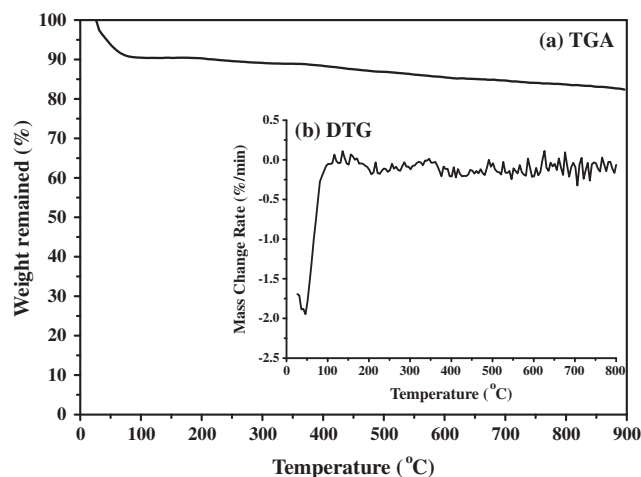**Fig. 2.** XRD patterns of as-synthesized MSP, as-synthesized MSP (AS) and washed MSP (AS) samples.

Fig. 3. (a) TGA and (b) DTG analyses of the washed MSP (AS).

Table 2
Physical properties of mesoporous and microporous adsorbents.

Sample name	S_{BET}[a] (m²/g)	d_{BJH}[b] (nm)	Vp[c] (cm³/g)
As-synthesized MSP (AS)	26	16.8	0.08
Washed MSP (AS)	585	9.1	1.24
Washed MSP	480	5.7	0.7
MCM-41	1101	3.0	0.99
SBA-15	745	6.5	1.10
Zeolite NaY	712	–	0.35
TEPA-MSP (AS)	54	8.7	0.22
TEPA-MCM-41	36	–	0.07
TEPA-SBA-15	40	6.0	0.11
TEPA-NaY	2.5	–	0.001

[a] BET surface area.
[b] Pore diameter calculated by BJH theory.
[c] Total pore volume.

decomposition of $(NH_4)_2SO_4$, which is typically thermally decomposed around 235–280 °C. This clearly reveals the absence of $(NH_4)_2SO_4$ salt in the washed MSP (AS) material. This is consistent with the XRD result which confirms the presence of pure siliceous material of the washed MSP (AS).

The N_2 adsorption–desorption isotherms of the washed MSP and MSP (AS) are presented in Fig. 4a. Both the washed samples show type IV isotherms of mesoporous material according to the IUPAC classification, featuring a narrow step due to capillary condensation of N_2 within the primary mesopores [25]. Furthermore, the isotherm of the washed MSP (AS) also shows the type H1 hysteresis loop, which is associated with the uniform pore channels. Fig. 4b displays the BJH pore size distribution of the washed MSP and MSP (AS) samples, where a significant pore enlargement is observed for washed MSP (AS) sample.

The effect of the salt templating medium on the physical properties such as BET specific surface area, total pore volume and BJH pore diameter derived from N_2 adsorption–desorption measurements are summarized in Table 2. Apparently, the as-synthesized MSP (AS) exhibits low surface area and tiny pore voids due to the occluded salt template. After the removal of salt matrix by aqueous washing, the specific surface area and the total pore volume of the washed MSP (AS) are drastically enhanced. In addition, the washed MSP (AS) shows higher surface area and larger pores as

compared to those of the washed MSP, which was prepared without the addition of $(NH_4)_2SO_4$. These results are quite conclusive in demonstrating that $(NH_4)_2SO_4$ salt can be employed as an effective template to support the mesostructure.

The possible pathway of formation of MSP and MSP (AS) materials via aerosol spray process is illustrated in Fig. 5. In the present study, sodium silicate solution extracted from photonic industrial waste powder is firstly acidified with the aid of hydrochloric acid to form polymeric silica sol. The NaCl crystallites are formed during sodium silicate acidification and embedded into MSP particles on aerosol process. As the precursor solution is aerosolized, the rapid evaporation of water drastically enhanced the silica polymerization and solidification of the salt to act as a template matrix to support the formation of porous structure. Finally, mesoporous silica particles with three-dimensional network can be obtained by subsequent aqueous washing process to completely remove the salt templates.

It is noteworthy that the mesoporous MSP (AS) is fabricated by employing dual templating mediums of NaCl and $(NH_4)_2SO_4$ simultaneously. Since $(NH_4)_2SO_4$ is more water soluble than NaCl, higher solubility favors nucleation and formation of bigger $(NH_4)_2SO_4$ nucleus in the droplets. Therefore, MSP (AS) material synthesized using dual salt templates shows larger pore diameter and pore volume than those of the MSP sample, which is synthesized in the presence of single template of NaCl.

The morphology of the washed MSP (AS) was revealed by SEM analysis depicted in Fig. 6a. It is observed that the washed MSP (AS) material is in spherical shape with particle size of ca. 1–1.5 μm. SEM image with higher magnification (Fig. 6b) further reveals that the washed MSP (AS) shows rough surface, which are assembled from primary nanoparticles with average size of ca. 25 nm. TEM image in Fig. 6c proves that the washed MSP (AS) particles are porous, appears to consist of interconnected network. Furthermore, the chemical composition of the washed MSP (AS) was analyzed by EDX analysis (Fig. 6d), where there are only Si and O elements observed (Cu peak from the TEM grid). This is in agreement with the XRD result, which confirms the presence of amorphous silica. Consequently, it can conclude that silica spherical particles with open mesoporous structure can be prepared using sodium silicate solution extracted from photonic industrial waste powder as the silica precursor via salt-templated aerosol route.

3.2. Application as adsorbents for CO_2 capture

Fig. 7 shows the time dependence of CO_2 uptake in the presence of 10% CO_2 at 60 °C for TEPA-functionalized MCM-41, SBA-15, MSP (AS) as well as zeolite NaY adsorbents. It can be found that the CO_2 uptake increased rapidly to more than 90% of the maximum uptake within the first 5 min of adsorption before reaching a constant
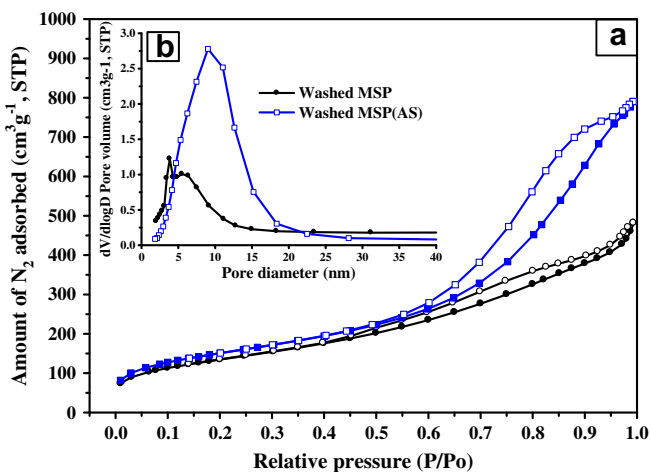

Fig. 4. (a) N_2 adsorption–desorption isotherms and (b) BJH pore diameter distributions of the washed MSP and MSP (AS) samples.
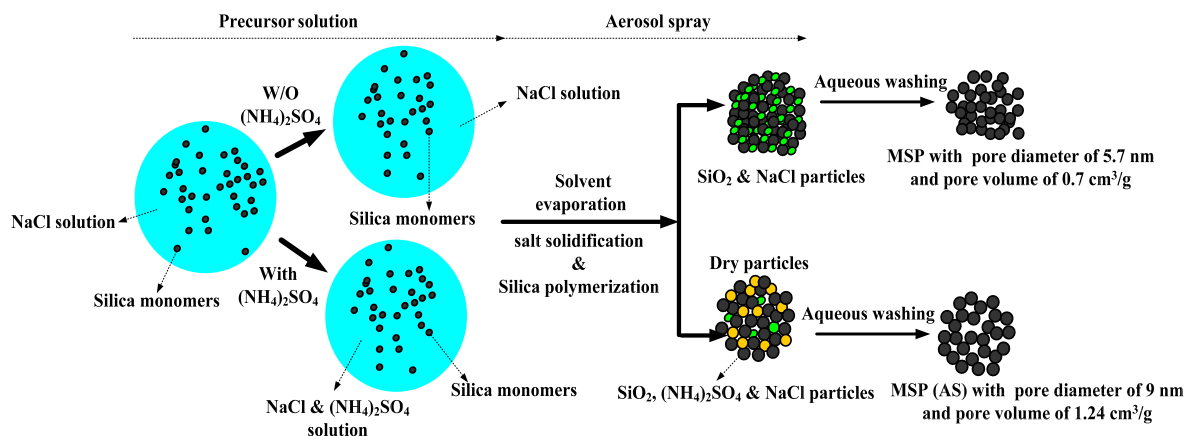
Fig. 5. Possible pathway for the formation of MSP and MSP (AS) samples through aerosol spray process.
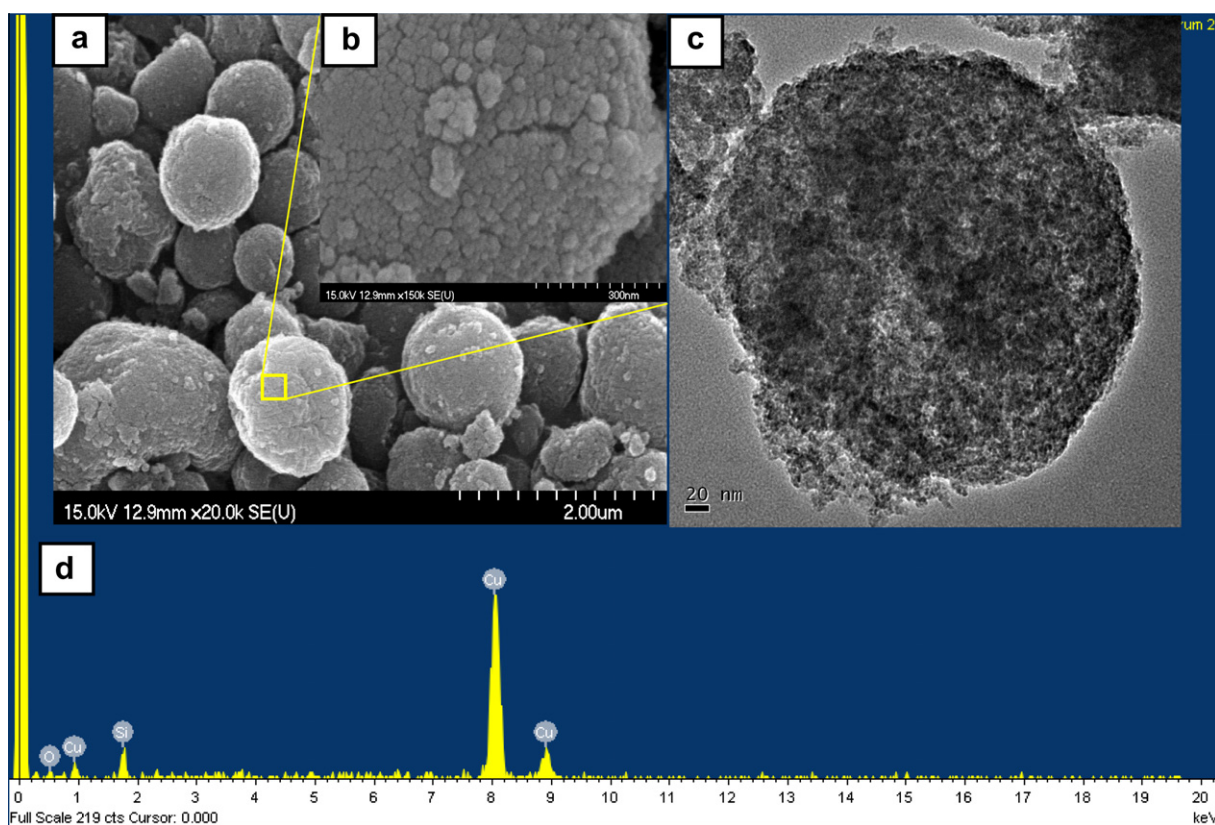

Fig. 6. SEM images (a) low-magnification, (b) high-magnification of the washed MSP (AS). (c) TEM image and (d) EDS spectrum of the washed MSP (AS).

equilibrium value for all adsorbents. The TEPA-MSP (AS) exhibits the highest CO_2 adsorption capacity, which could achieve 127 mg CO_2/g adsorbent, followed by the TEPA-SBA-15 (117 mg CO_2/g adsorbent), TEPA-MCM-41 (112 mg CO_2/g adsorbent) and TEPA-NaY (96 mg CO_2/g adsorbent). It is noteworthy that the adsorption capacity sequence coincides with the order of pore diameter and total pore volume of the parent silica supports.

The difference in the CO_2 uptake between TEPA-MSP (AS), TEPA-SBA-15, TEPA-MCM-41 and TEPA-NaY can be elucidated by their N_2 adsorption–desorption isotherms as shown in Fig. 8a and b as well as their pore structure data listed in Table 2. As shown in Fig. 8a, the parent MCM-41, SBA-15 and MSP (AS) all show type IV isotherms of mesoporous materials, while type I isotherm of microporous material is observed for raw NaY. After functionalized with TEPA, it was

found from Fig. 8b that both TEPA-MCM-41 and TEPA-NaY adsorbents exhibit type II isotherm, which is a typical indication of non-porous material. This implies that both MCM-41 and NaY supports were fully filled with 50 wt.% of TEPA reagents. On the other hand, both TEPA-MSP (AS) and TEPA-SBA-15 samples show sharp capillary condensation steps with well-resolved hysteresis loops, suggesting that the intrinsic mesostructures of the MSP (AS) and SBA-15 were still partially retained after TEPA loading.

Because the density of TEPA is about 0.99 cm^3/g and the total pore volumes of parent MSP (AS), SBA-15, MCM-41 and NaY are 1.24 cm^3/g, 1.10 cm^3/g, 0.99 cm^3/g and 0.35 cm^3/g, the maximum TEPA loading expected to load inside the channels of MSP (AS), SBA-15, MCM-41 and NaY is 56%, 53%, 50% and 26%, respectively. It is reported that more efficient contact between the CO_2 gas
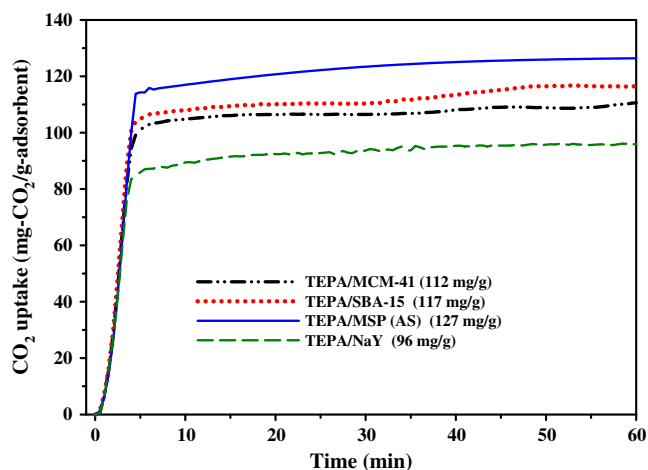
Fig. 7. Comparison on CO_2 uptakes of TEPA loaded on MCM-41, SBA-15, MSP (AS) and NaY zeolite samples.

materials can increase the adsorption capacity, the pore diameter and pore volume of the support seem to largely influence the adsorption capacity. The results of Xu et al. [33] seem to be in consistent with the results of this study. The only exception shown in Table 3 is that under similar conditions, TEPA-KIT-6 exhibited an adsorption capacity of 129 mg CO_2/g adsorbent, which is slightly higher than that of TEPA-MSP (AS). This could be due to that KIT-6 with high surface area and uniform 3D pore arrangement could promote better dispersion of amines. These two effects may combine together and result in further increment of the adsorption capacity.

Fig. 9 depicts the effect of CO_2 concentration on the adsorption performance of TEPA-MSP (AS). It is observed that TEPA-MSP (AS) exhibits a high adsorption capacity at low CO_2 concentration, and the value achieved using 10% CO_2 (127 mg CO_2/g adsorbent) is only slightly less than that for pure CO_2 (138 mg CO_2/g adsorbent). This clearly suggests that the TEPA-MSP (AS) adsorbent has a high selectivity towards CO_2. The high adsorption capacity, especially at low CO_2 concentration implies that the TEPA-MSP (AS) adsorbent may be useful for practical applications, such as those relevant in flue gas and for capture CO_2 from ambient air [34,35].

3.3. Comparison of MSP (AS), MCM-41 and SBA-15

TEPA-related materials used for CO_2 adsorption from the literature and this work in terms of their starting precursors, manufacture process as well as CO_2 adsorption performance are summarized in Table 3. It is observed that under the same conditions, TEPA-MSP (AS) adsorbent has an excellent adsorption performance at low CO_2 concentration as compared to other adsorbents.

To date, research works on the preparation of mesoporous silica materials including MCM-41, SBA-15 and KIT-6 are manufactured via conventional hydrothermal process, which require long and tedious batch process time of several days. A subsequent thermal process is also required to remove the organic surfactants from the silica/surfactant hybrids, which would further increase the manufacturing costs and energy penalty. Furthermore, it has been reported that conventional MCM-41 and SBA-15 materials with rod- or flake-shaped particles tend to have low bulk density, which would lead to higher pressure drop for obtaining the same mass

and the impregnated TEPA could be achieved when a small space is still left inside the pores of the mesoporous silica after TEPA loading [31]. As a result, the MCM-41 and NaY had lower CO_2 adsorption capacities due to the fact that they had smaller pore volumes, which may result in more constricted or blocked pores in the adsorbents.

Furthermore, since both the pores of MSP (AS) and SBA-15 were not completely filled by TEPA, there are enough accessible spaces in TEPA-MSP (AS) and TEPA-SBA-15 samples. Therefore, it could be speculated that the pore volume was not a main parameter which affected the CO_2 capturing performance when the pores were not completely occupied. Recently Yan et al. [32] demonstrated that the CO_2 uptake increased with the increasing pore size of mesoporous substrates. Thus, the MSP (AS) with larger pore diameter could facilitate more TEPA into the pore channels more easily, which would lead to higher CO_2 adsorption performance than that of SBA-15 with smaller pore diameter. Xu et al. [33] employed polyethylenimine (PEI)-impregnated MCM-41 for CO_2 adsorption. They claimed that although the dispersion of PEI on the high surface area

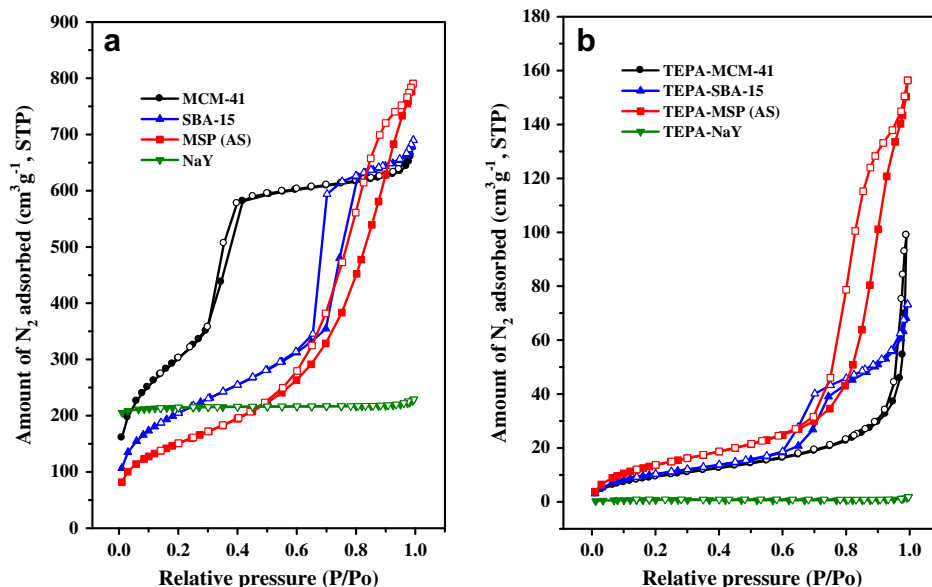**Fig. 8.** N_2 adsorption–desorption isotherms (a) parent MCM-41, SBA-15, MSP (AS) and NaY zeolite and (b) TEPA loaded on MCM-41, SBA-15, MSP (AS) and NaY zeolite samples.

Table 3
TEPA-related adsorbents for CO_2 capture from previous literature and our work.

Support	Precursor	Synthesis process	Process time	S_{BET} (m²/g)	d_{BJH} (nm)	Vp (cm³/g)	Capacity (mg/g)	Relative price of chemicals[a]	Reference
KIT-6	Tetraethylorthosilicate + P123	Batch process	49 h process + calcination	943	6.0	1.0	129	–	[40]
SBA-15	Sodium silicate + P123	Batch process	24 h process + 6 h calcination	745	6.5	1.10	117	0.41	This work
MCM-41	Sodium silicate + CTAB	Batch process	36 h process + 6 h calcination	1101	3.0	0.99	112	1.00	This work
MSP (AS)	Waste powder + $(NH_4)_2SO_4$	Continuous process	4 s process + washing	585	9.1	1.24	127	0.3	This work

[a] The relative prices of chemicals were calculated based on the ratio of the purchase price of chemicals used for manufacturing the adsorbents to that for manufacturing the MCM-41. The treatment and disposal costs of the photonic waste powder were not included, which should further reduce the manufacture costs of the mesoporous materials when using the waste powder as the precursor.
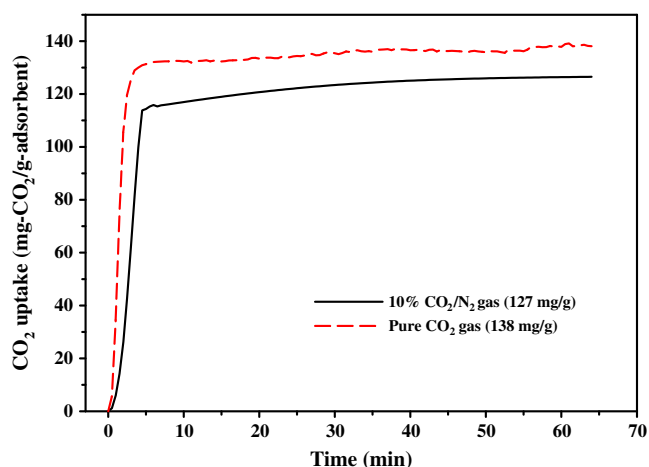

Fig. 9. CO_2 adsorption performance of TEPA-MSP (AS) with 10% and pure CO_2 feed gas at 60 °C.

adsorption capacity of adsorbent [36]. The use of spherical MSP (AS) particles with higher volume-based adsorption capacity as supports of adsorbents can significantly reduce the adsorber volume of CO_2, and this has been another important issue that needs to be considered for field application.

It can be seen from Table 3 that the use of waste material and soluble salt instead of costly silica source and organic surfactants drastically reduces the manufacturing expenses of mesoporous silica materials and this would be one of the most important considerations for industrial applications. Moreover, there have been reports on the development of aerosol processing apparatus suitable for rapid mass production and industrial uses [37–39]. Therefore, the MSP (AS) material shows several advantages in terms of low-cost synthetic process, fast production rate and high CO_2 adsorption capacity. It could be considered as a potential and competitive adsorbent for the CO_2 capture from flue gas. In this study, this novel process, which can improve cost effectiveness for the mass production of valuable mesoporous silica materials from cheap and abundant resources through rapid aerosol process, is truly beneficial from the viewpoint of economical use of photonic industrial waste powder.

4. Conclusions

This work provides a simple and fast approach for developing economically effective mesoporous siliceous adsorbents using photonic industrial waste powder as the silica source, along with inorganic salt as the templating medium via aerosol process. The

obtained mesoporous MSP (AS) has high specific surface area, large pore diameter and large pore volume. Besides, the MSP (AS) material in this study is a better support of adsorbent for CO_2 capture, which has a higher CO_2 adsorption capacity of 127 mg/g adsorbent than that of MCM-41 and SBA-15 manufactured using pure silica chemicals as well as commercial zeolite NaY. Compared to the conventional mesoporous MCM-41 and SBA-15, the spherical MSP (AS) possesses advantages of rapid synthesis, low manufacturing costs and high adsorption capacity. In addition, it can reduce the waste production rate as well as the consumption rate of natural silica resource. Thus the MSP (AS) can be a high cost-effective adsorbent for the CO_2 greenhouse gas capture from flue gas.

Acknowledgment

References

[1] A.B. Rao, E.S. Rubin, A technical, economic, and environmental assessment of amine-based CO_2 capture technology for power plant greenhouse gas control, Environ. Sci. Technol. 36 (2002) 4467–4475.
[2] J.D. Figueroa, T. Fout, S. Plasynski, H. McIlvried, R.D. Srivastava, Advances in CO_2 capture technology – the US Department of Energy's Carbon Sequestration Program, Int. J. Greenhouse Gas Control 2 (2008) 9–20.
[3] J.C. Fisher II, J. Tanthana, S.S.C. Chuang, Oxide-supported tetraethylenepentamine for CO_2 capture, Environ. Prog. Sustain. Energy 28 (2009) 589–598.
[4] R.P. Ribeiro, T.P. Sauer, F.V. Lopes, R.F. Moreira, C.A. Grande, A.E. Rodrigues, Adsorption of CO_2, CH_4, and N_2 in activated carbon honeycomb monolith, J. Chem. Eng. Data 53 (2008) 2311–2317.
[5] S.-C. Hsu, C. Lu, F. Su, W. Zeng, W. Chen, Thermodynamics and regeneration studies of CO_2 adsorption on multiwalled carbon nanotubes, Chem. Eng. Sci. 65 (2010) 1354–1361.
[6] M. Bhagiyalakshmi, J.Y. Lee, H.T. Jang, Synthesis of mesoporous magnesium oxide: its application to CO_2 chemisorption, Int. J. Greenhouse Gas Control 4 (2010) 51–56.
[7] Z. Zhao, X. Cui, J. Ma, R. Li, Adsorption of carbon dioxide on alkali-modified zeolite 13X adsorbents, Int. J. Greenhouse Gas Control 1 (2007) 355–359.
[8] A.L. Chaffee, G.P. Knowles, Z. Liang, J. Zhang, P. Xiao, P.A. Webley, CO_2 capture by adsorption: materials and process development, Int. J. Greenhouse Gas Control 1 (2007) 11–18.
[9] W.-J. Son, J.-S. Choi, W.-S. Ahn, Adsorptive removal of carbon dioxide using polyethyleneimine-loaded mesoporous silica materials, Micropor. Mesopor. Mater. 113 (2008) 31–40.
[10] A. Sayari, M. Kruk, M. Jaroniec, I.L. Moudrakovski, New approaches to pore size engineering of mesoporous silicates, Adv. Mater. 10 (1998) 1376–1379.
[11] H.T. Jang, Y. Park, Y.S. Ko, J.Y. Lee, B. Margandan, Highly siliceous MCM-48 from rice husk ash for CO_2 adsorption, Int. J. Greenhouse Gas Control 3 (2009) 545–549.
[12] H.-L. Chang, C.-M. Chun, I.A. Aksay, W.-H. Shih, Conversion of fly ash into mesoporous aluminosilicate, Ind. Eng. Chem. Res. 38 (1999) 973–977.
[13] Y. Liu, Y. Guo, Y. Zhu, D. An, W. Gao, Z. Wang, Y. Ma, Z. Wang, A sustainable route for the preparation of activated carbon and silica from rice husk ash, J. Hazard. Mater. 186 (2011) 1314–1319.

[14] X. Ma, B. Zhou, W. Gao, Y. Qu, L. Wang, Z. Wang, Y. Zhu, A recyclable method for production of pure silica from rice hull ash, Powder Technol. 217 (2012) 497–501.

[15] D. An, Y. Guo, Y. Zhu, Z. Wang, A green route to preparation of silica powders with rice husk ash and waste gas, Chem. Eng. J. 162 (2010) 509–514.

[16] Y. Kuwahara, T. Ohmichi, T. Kamegawa, K. Mori, H. Yamashita, A novel conversion process for waste slag: synthesis of a hydrotalcite-like compound and zeolite from blast furnace slag and evaluation of adsorption capacities, J. Mater. Chem. 20 (2010) 5052–5062.

[17] L.-Y. Lin, J.-T. Kuo, H. Bai, Silica materials recovered from photonic industrial waste powder: its extraction, modification, characterization and application, J. Hazard. Mater. 192 (2011) 255–262.

[18] C. Boissiere, D. Grosso, A. Chaumonnot, L. Nicole, C. Sanchez, Aerosol route to functional nanostructured inorganic and hybrid porous materials, Adv. Mater. 23 (2011) 599–623.

[19] J.H. Bang, K.S. Suslick, Applications of ultrasound to the synthesis of nanostructured materials, Adv. Mater. 22 (2010) 1039–1059.

[20] S.H. Kim, B.Y.H. Liu, M.R. Zachariah, Ultra high surface area nanoporous silica particles via an aero-sol–gel process, Langmuir 20 (2004) 2523–2526.

[21] T. Kimura, K. Kato, Y. Yamauchi, Temperature-controlled and aerosol-assisted synthesis of aluminium organophosphonate spherical particles with uniform mesopores, Chem. Commun. (2009) 4938.

[22] Y. Lu, H. Fan, A. Stump, T.L. Ward, T. Rieker, C.J. Brinker, Aerosol-assisted self-assembly of mesostructured spherical nanoparticles, Nature 398 (1999) 223–226.

[23] Y. Lu, H. Fan, N. Doke, D.A. Loy, R.A. Assink, D.A. LaVan, C.J. Brinker, Evaporation-induced self-assembly of hybrid bridged silsesquioxane film and particulate mesophases with integral organic functionality, J. Am. Chem. Soc. 122 (2000) 5258–5261.

[24] C. Urata, Y. Yamauchi, Y. Aoyama, J. Imasu, S. Todoroki, Y. Sakka, S. Inoue, K. Kuroda, Fabrication of hierarchically porous spherical particles by assembling mesoporous silica nanoparticles via spray drying, J. Nanosci. Nanotechnol. 8 (2008) 3101–3105.

[25] L.-Y. Lin, H. Bai, Continuous generation of mesoporous silica particles via the use of sodium metasilicate precursor and their potential for CO_2 capture, Micropor. Mesopor. Mater. 136 (2010) 25–32.

[26] S.H. Kim, B.Y.H. Liu, M.R. Zachariah, Synthesis of nanoporous metal oxide particles by a new inorganic matrix spray pyrolysis method, Chem. Mater. 14 (2002) 2889–2899.

[27] C. Jo, K. Kim, R. Ryoo, Syntheses of high quality KIT-6 and SBA-15 mesoporous silicas using low-cost water glass, through rapid quenching of silicate structure in acidic solution, Micropor. Mesopor. Mater. 124 (2009) 45–51.

[28] R. Kiyoura, K. Urano, Mechanism, kinetics, and equilibrium of thermal decomposition of ammonium sulfate, Ind. Eng. Chem. Proc. Des. Dev. 9 (1970) 489–494.

[29] P.B. Sarawade, J.-K. Kim, A. Hilonga, H.T. Kim, Recovery of high surface area mesoporous silica from waste hexafluorosilicic acid (H_2SiF_6) of fertilizer industry, J. Hazard. Mater. 173 (2010) 576–580.

[30] K. Liu, Q. Feng, Y. Yang, G. Zhang, L. Ou, Y. Lu, Preparation and characterization of amorphous silica nanowires from natural chrysotile, J. Non-Cryst. Solids 353 (2007) 1534–1539.

[31] C. Chen, W.-J. Son, K.-S. You, J.-W. Ahn, W.-S. Ahn, Carbon dioxide capture using amine-impregnated HMS having textural mesoporosity, Chem. Eng. J. 161 (2010) 46–52.

[32] X. Yan, L. Zhang, Y. Zhang, K. Qiao, Z. Yan, S. Komarneni, Amine-modified mesocellular silica foams for CO_2 capture, Chem. Eng. J. 168 (2011) 918–924.

[33] X. Xu, C. Song, J.M. Andresen, B.G. Miller, A.W. Scaroni, Novel polyethylenimine-modified mesoporous molecular sieve of MCM-41 type as high-capacity adsorbent for CO_2 capture, Energy Fuels 16 (2002) 1463–1469.

[34] X. Wang, X. Ma, V. Schwartz, J.C. Clark, S.H. Overbury, S. Zhao, X. Xu, C. Song, A solid molecular basket sorbent for CO_2 capture from gas streams with low CO_2 concentration under ambient conditions, Phys. Chem. Chem. Phys. 14 (2012) 1485.

[35] Y. Liu, Q. Ye, M. Shen, J. Shi, J. Chen, H. Pan, Y. Shi, Carbon dioxide capture by functionalized solid amine sorbents with simulated flue gas conditions, Environ. Sci. Technol. 45 (2011) 5710–5716.

[36] C. Hung, H. Bai, M. Karthik, Ordered mesoporous silica particles and Si-MCM-41 for the adsorption of acetone: a comparative study, Sep. Purif. Technol. 64 (2009) 265–272.

[37] Y. Yamauchi, P. Gupta, K. Sato, N. Fukata, S. Todoroki, S. Inoue, S. Kishimoto, Industrial mass-production of mesoporous silica spherical particles by a spray-drying process: investigation of synthetic conditions, J. Ceram. Soc. Jpn. 117 (2009) 198–202.

[38] Y. Yamauchi, T. Kimura, Aerosol-assisted rapid fabrication of well-dispersed and highly doped titanium-containing mesoporous silica microspheres, Chem. Lett. 37 (2008) 892–893.

[39] Y. Yamauchi, N. Suzuki, K. Sato, N. Fukata, M. Murakami, T. Shimizu, Active mercury(II) ion removal: stoichiometrically controlled thiol-functionalized mesoporous silica by a mass production spray dry system, Bull. Chem. Soc. Jpn. 82 (2009) 1039–1043.

[40] Y. Liu, J. Shi, J. Chen, Q. Ye, H. Pan, Z. Shao, Y. Shi, Dynamic performance of CO_2 adsorption with tetraethylenepentamine-loaded KIT-6, Micropor. Mesopor. Mater. 134 (2010) 16–21.